

Published in final edited form as:

*Bioorg Med Chem Lett.* 2010 October 1; 20(19): 5662–5665. doi:10.1016/j.bmcl.2010.08.031.

## Unusual Antimalarial Meroditerpenes from Tropical Red Macroalgae

E. Paige Stout<sup>a</sup>, Jacques Prudhomme<sup>c</sup>, Karine Le Roch<sup>c</sup>, Craig R. Fairchild<sup>d</sup>, Scott G. Franzblau<sup>e</sup>, William Aalbersberg<sup>f</sup>, Mark E. Hay<sup>b</sup>, and Julia Kubanek<sup>a,b,\*</sup>

<sup>a</sup>School of Chemistry and Biochemistry, Georgia Institute of Technology, Atlanta, GA, USA 30332

<sup>b</sup>School of Biology, Georgia Institute of Technology, Atlanta, GA, USA 30332

<sup>c</sup>Department of Cell Biology and Neuroscience, University of California Riverside, Riverside, CA, USA 92521

<sup>d</sup>Bristol-Myers Squibb Pharmaceutical Research Institute, Princeton, NJ, USA 08543

<sup>e</sup>Institute for Tuberculosis Research, College of Pharmacy, University of Illinois at Chicago, Chicago, IL, USA 60612

<sup>f</sup>Institute of Applied Sciences, University of the South Pacific, Suva, Fiji

### Abstract

Three antimalarial meroditerpenes have been isolated from two Fijian red macroalgae. The absolute stereochemistry of callophycolide A (**1**), a unique macrolide from *Callophycus serratus*, was determined using a combination of Mosher's ester analysis, circular dichroism analysis with a dimolybdenum tetraacetate complex, and conformational analysis using NOEs. In addition, two known tocopherols,  $\beta$ -tocopherylhydroquinone (**4**) and  $\delta$ -tocopherylhydroquinone (**5**), were isolated from *Amphiroa crassa*. By oxidizing **5** to the corresponding  $\delta$ -tocopherylquinone (**6**), antimalarial activity against the human malaria parasite *Plasmodium falciparum* was increased by more than 20-fold.

© 2010 Elsevier Ltd. All rights reserved.

\*Corresponding author. Mailing address: 310 Ferst Drive NW, Atlanta, GA 30332-0230, USA, Phone: (404) 894-8424, Fax: (404) 385-4440, julia.kubanek@biology.gatech.edu.

**Publisher's Disclaimer:** This is a PDF file of an unedited manuscript that has been accepted for publication. As a service to our customers we are providing this early version of the manuscript. The manuscript will undergo copyediting, typesetting, and review of the resulting proof before it is published in its final citable form. Please note that during the production process errors may be discovered which could affect the content, and all legal disclaimers that apply to the journal pertain.

#### Supplementary Data

Experimental details and 1 and 2-D NMR spectroscopic data for **1** and **4–5** are available free of charge via the Internet.

#### Compound data

**Callophycolide A (1):** pale yellow oil (4.0 mg, 0.021% dry mass);  $[\alpha]_D^{24} +200$  (c 0.01, MeOH); UV (MeOH)  $\lambda_{max}$  (log  $\epsilon$ ) 260 (4.06) nm; <sup>1</sup>H, <sup>13</sup>C, NOE, COSY, HSQC-TOCSY, and HMBC NMR data, see Supplementary Data; HRESIMS  $[M + H]^+$   $m/z$  427.2825 (calcd for C<sub>27</sub>H<sub>39</sub>O<sub>4</sub>, 427.2842) and  $[M + Na]^+$   $m/z$  449.2623 (calcd for C<sub>27</sub>H<sub>38</sub>O<sub>4</sub>Na, 449.2668).

**$\beta$ -Tocopherylhydroquinone (4):** clear oil (1.2 mg, 0.003% plant dry mass);  $[\alpha]_D^{24} +2.2$  (c 0.06, MeOH); UV (MeOH)  $\lambda_{max}$  (log  $\epsilon$ ) 255 (3.93) nm; <sup>1</sup>H, <sup>13</sup>C, COSY, and HMBC NMR data, see Supplementary Data; HRESIMS  $[M-H-H_2O]^-$   $m/z$  415.3553 (calcd for C<sub>28</sub>H<sub>47</sub>O<sub>2</sub>, 415.3576).

**$\delta$ -Tocopherylhydroquinone (5):** brown oil (2.8 mg, 0.006% plant dry mass);  $[\alpha]_D^{24} +1.3$  (c 0.14, MeOH); UV (MeOH)  $\lambda_{max}$  (log  $\epsilon$ ) 255 (3.56) nm; <sup>1</sup>H, <sup>13</sup>C, COSY, and HMBC NMR data, see Supplementary Data; HRESIMS  $[M-H-H_2O]^-$   $m/z$  401.3414 (calcd for C<sub>27</sub>H<sub>45</sub>O<sub>2</sub>, 401.3419);  $[2M-H-2H_2O]^-$   $m/z$  803.6876 (calcd for C<sub>54</sub>H<sub>91</sub>O<sub>4</sub>, 803.6917).

## Keywords

*Callophycus serratus*; *Amphiroa crassa*; natural product; drug discovery; red macroalgae

Natural products have been the source of the most successful antimalarial drugs to date, including most notably the quinines and artemisinins.<sup>1,2</sup> The design and development of many synthetic antimalarial drugs has largely been inspired by these and other antimalarial natural products.<sup>1</sup> Thus, the discovery of novel chemistry from natural sources could provide new scaffolds for the development of much needed antimalarial treatments. We previously discovered a structurally-novel class of brominated diterpenoid macrolides, called bromophycolides, from the Fijian red macroalga *Callophycus serratus*,<sup>3-4</sup> and several bromophycolides exhibited submicromolar activity against the human malaria parasite *Plasmodium falciparum*.<sup>5-6</sup> Our continued efforts to uncover antimalarial natural products from understudied tropical red macroalgae led us to explore potent activity from two red algae in our library, thus leading to the identification of an unusual non-brominated macrolide we named callophycolide A (**1**) and two known tocopherols,  $\beta$ -tocopherylhydroquinone (**4**) and  $\delta$ -tocopherylhydroquinone (**5**) from the coralline alga *Amphiroa crassa*.

*Callophycus serratus* (family Solieriaceae, order Gigartinales, class Rhodophyceae, phylum Rhodophyta) was collected at depths of 2–3 m from Yanuca in the Fiji Islands (18° 23' 57" S, 177° 57' 59" E), and *Amphiroa crassa* (family Corallinaceae, order Corallinales, class Florideophyceae, phylum Rhodophyta) was collected at a depth of 20 m from the Coral Coast, Fiji (18° 12' 15" S, 177° 39' 35" W). Frozen *C. serratus* and *A. crassa* were each extracted with MeOH and MeOH:DCM (1:1, 1:2) and subjected to liquid partitioning between MeOH:H<sub>2</sub>O (9:1) and petroleum ether. The MeOH:H<sub>2</sub>O ratio of each species' aqueous fraction was then adjusted to 3:2 and partitioned against chloroform. The chloroform-soluble fraction for each species was then separated with multiple rounds of reversed-phase C<sub>18</sub> HPLC (Alltech Alltima C<sub>18</sub>, 5  $\mu$ m, 10  $\times$  250 mm) with a gradient of MeCN (aq) to yield **1** from *C. serratus* and **4-5** from *A. crassa*.

Unlike previously isolated bromophycolides<sup>3-6</sup>, callophycolide A (**1**) did not display a characteristic brominated isotopic pattern with HRESIMS, but showed an [M + H]<sup>+</sup> *m/z* of 427.2825, appropriate for a formula of C<sub>27</sub>H<sub>38</sub>O<sub>4</sub>. The *p*-hydroxybenzoate segment common to all reported *Callophycus serratus* secondary metabolites<sup>3-7</sup> remained intact, apparent from the <sup>13</sup>C and <sup>1</sup>H NMR chemical shifts for positions 3 ( $\delta_C$  131.1;  $\delta_H$  7.85), 21 ( $\delta_C$  129.6;  $\delta_H$  7.73), 22 ( $\delta_C$  114.8;  $\delta_H$  6.78), and 23 ( $\delta_C$  158.0; OH  $\delta_H$  5.83). HMBC correlations from H<sub>2</sub>-5 ( $\delta$  3.17, 3.49) to C-3, C-4 ( $\delta$  127.7), and C-23 connected the C-5 methylene to the *p*-hydroxybenzoate fragment, as in bromophycolides, but surprisingly C-5 was not connected to a substituted cyclohexene. Instead, a linear isoprene unit was established through COSY correlations between both H<sub>2</sub>-5 protons and H-6 ( $\delta$  5.45), as well as HMBC correlations from Me-24 ( $\delta$  1.60) to C-6 ( $\delta$  122.7), C-7 ( $\delta$  136.8), and C-8 ( $\delta$  39.3). COSY correlations failed to establish the vicinal relationship of H<sub>2</sub>-8 ( $\delta$  2.17, 2.27) and H<sub>2</sub>-9 ( $\delta$  2.15, 2.23) due to substantial chemical shift overlap; instead, HSQC-TOCSY correlations were used to connect well-resolved carbons at C-8 and C-9 ( $\delta$  23.8; Figure 1). COSY correlations between both H<sub>2</sub>-9 protons and H-10 ( $\delta$  5.19) and HMBC correlations from Me-25 ( $\delta$  1.59) to C-10 ( $\delta$  123.5), C-11 ( $\delta$  135.2), and C-12 ( $\delta$  35.8) connected a second isoprene unit within **1**. HMBC correlations from H-14 ( $\delta$  4.75) to C-1 ( $\delta$  169.2), C-12 ( $\delta$  35.8), C-13 ( $\delta$  29.2), C-15 ( $\delta$  74.8), and Me-26 ( $\delta_C$  22.0) provided strong evidence in support of a macrocyclic lactone framework and accounted for a third isoprene fragment. Me-26 ( $\delta_H$  1.16) showed strong HMBC signals to C-14 ( $\delta$  82.1), C-15, and C-16 ( $\delta$  40.0), while vicinal COSY correlations established a C-16—C-17—C-18 connectivity. Allylic coupling was observed with weak COSY correlations between H-18 ( $\delta$  5.10) and both Me-20 ( $\delta$  1.66) and Me-27 ( $\delta$  1.60), establishing the diterpene head. This structural feature was

further confirmed by HMBC correlations from both Me-20 and Me-27 to C-18 ( $\delta$  124.3), C-19 ( $\delta$  131.8), and to each other, completing the planar connectivity of **1**.

ROESY data were used to assign the configurations of the olefins within the macrocyclic ring. NOEs observed between H-6 and both H<sub>2</sub>-8 protons and between H<sub>b</sub>-5 ( $\delta$  3.49) and Me-24 ( $\delta$  1.60) supported an *E* configuration for  $\Delta$ 6<sup>7</sup>. Similarly, ROESY correlations between H-10 ( $\delta$  5.19) and H<sub>a</sub>-12 ( $\delta$  1.87) as well as between H<sub>b</sub>-9 ( $\delta$  2.23) and Me-25 ( $\delta$  1.59) suggested an *E* configuration for  $\Delta$ <sup>10,11</sup> (Figure 1b).

Absolute configuration at C-14 was determined by analysis of Mosher ester data<sup>8</sup> derived from the methylated hydrolysis product **7** (Figure 2a). Hydrolyzed product **7** was acylated with each of *R*-(-)- and *S*-(+)- $\alpha$ -methoxy- $\alpha$ -(trifluoromethyl)phenylacetyl chloride (MTPA-Cl) to produce the corresponding *S*- and *R*-MTPA esters **7a** and **7b**, respectively. Analysis of the <sup>1</sup>H NMR and HSQC-TOCSY spectra obtained for both esters permitted the assignment of the proton chemical shifts in proximity of the esterified carbon. Calculation of the  $\Delta\delta_{S-R}$  values established the absolute configuration of C-14 as *S* based upon empirical rules proposed by Ohtani *et al.*<sup>8</sup> (Figure 2b).

Solution of the configuration at C-15 proved to be challenging relative to other stereocenters in **1**. Frelek *et al.* reported a circular dichroism (CD) spectroscopic method for determining the absolute configuration of restricted and flexible vicinal diols complexed with dimolybdenum tetraacetate.<sup>9–10</sup> After ligation to Mo<sub>2</sub>, free-rotation about flexible diols is substantially reduced due to steric requirements of the transition metal complex. The energetically preferred conformation of a flexible diol ligated to Mo<sub>2</sub> in a bidentate fashion is an antiperiplanar orientation of the O—C—C—R groups, with the bulky R-groups pointing away from the Mo<sub>2</sub> complex and the vicinal diols in a *gauche* conformation.<sup>10</sup> The CD spectrum of the *in situ* formed Mo<sub>2</sub> complex with **7** showed a negative Cotton effect at 310 nm, which corresponded to a negative O—C—C—O dihedral angle (Figure 3) as predicted by the helicity rule proposed by Frelek *et al.*<sup>9</sup> Molecular modeling was performed with HyperChem using the molecular mechanics MM+ force field method and conjugate gradient Polak Ribiere algorithm with RMS gradient of 0.001 kcal/Å·mol as described in Górecki *et al.*<sup>10</sup> Molecular modeling of a 14*S*, 15*S* configuration in accordance with the lowest energy conformation predicted a positive O—C—C—O dihedral angle, ruling out this diastereomer and suggesting a 14*S*, 15*R* configuration, whose preferred conformation of the dimolybdenum complex could have yielded either a positive or negative torsional angle. A stable conformation of **1** could involve intramolecular hydrogen bonding between the C-15 hydroxy and C-1 carbonyl, as predicted by molecular modeling (Supplemental Data). This places the C-15 hydroxy *anti* to H-14 which is supported by NOEs observed between H-14 and both H<sub>b</sub>-16 ( $\delta$  1.52) and Me-26; however this conformation is feasible for both 15*R* and 15*S*. An NOE correlation from H<sub>b</sub>-16 to H<sub>b</sub>-13 ( $\delta$  2.03) could differentiate between a 15*R* or 15*S* configuration (Figure 4), and inspection of 1D NOE spectra (irradiating H<sub>b</sub>-16, acquired at -10 °C) showed the presence of this correlation. Lack of NOEs between H<sub>2</sub>-13 protons and Me-26 implied an *anti* conformation of these groups and further supported a 15*R* stereochemical assignment (Figure 4). Overall, the combination of Mosher's ester analysis, CD analysis with a dimolybdenum tetraacetate complex, and conformational analysis using NOEs argue strongly for an absolute stereochemistry of 14*S*, 15*R* for **1**.

Previously reported bromophycolides<sup>3–6</sup> (e.g., bromophycolide A, **2**) and related non-macrocyclic callophycoids and callophycols<sup>7</sup> exhibit antimalarial IC<sub>50</sub> values ranging from 0.3 to >100  $\mu$ M, providing a detailed structure-activity relationship (SAR) analysis for this class of compounds.<sup>6</sup> The identification of **1** provides additional insight into the SAR for 33 known *C. serratus* metabolites, in that **1** retains moderate antimalarial activity (IC<sub>50</sub> = 5.2  $\mu$ M, Table 1) despite the complete absence of bromine atoms, similar to debromophycolide A

(3), whose antimalarial IC<sub>50</sub> is > 100 M. Furthermore, **1** has a carbon skeleton different than other bromophycolides, although its skeleton is not unprecedented and is shared with tocopherols.<sup>11</sup> The lactonization pattern through C-14 in **1** is unique, and the absence of a substituted cyclohexene ring (compared to **2**, IC<sub>50</sub> = 0.7 μM) suggests that this ring is not essential but can enhance antimalarial activity. Callophycolide A (**1**) was tested against 12 human cancer cell lines, exhibiting only modest cytotoxicity against most cell lines (IC<sub>50</sub> values ranging from 16–22 μM); the two most sensitive cell lines, CCRF-CEM (leukemia tumor cells) and SHP-77 (lung tumor cells), showed moderate IC<sub>50</sub> values of 7.5 and 9.2 μM, respectively. Callophycolide A (**1**) inhibited bacterial growth in the low micromolar range but was ineffective at deterring growth of human pathogenic fungi (Table 1).

Purified from extracts of *A. crassa*, tocopheryhydroquinones **4–5** were identified by a detailed analysis of their 1- and 2D NMR and MS spectral data and compared to related tocopherols previously reported.<sup>12–13</sup> While <sup>1</sup>H and <sup>13</sup>C NMR spectral data are available in the literature for vitamin E and related tocopherols, complete spectral data for **4–5** were lacking. Therefore, we provide full NMR spectral data for **4–5** in the present study (see Supplementary Data).

Tocopherols have been isolated and characterized from various brown algae including *Sargassum fallax*<sup>13</sup> and *Cystoseira stricta*.<sup>14</sup> but the identification of **4–5** represents the first isolation of tocopherols from red algae. This class of molecules has been shown to have a variety of functions in terrestrial vascular plants, including scavenging lipid peroxy radicals and preventing propagation of lipid peroxidation in membranes; protecting lipids and other membrane components by quenching and reacting with singlet oxygen and thus providing photoprotection for chloroplasts; and increasing membrane rigidity.<sup>15</sup> While a number of tocopherol derivatives have been isolated from brown macroalgae, their ecological functions are unclear. These compounds may function similarly as in vascular plants given the high exposure of many macroalgae to UV radiation, however this hypothesis has not been tested.

The biomedical potential of tocopherols and related compounds mainly relate to their antioxidant activities, as these compounds are well established in their radical scavenging activity.<sup>16</sup> Hydroquinones **4–5** showed weak activity against *P. falciparum* (IC<sub>50</sub> values of 190 and 220 μM for **4** and **5**, respectively, Table 1), but oxidation of **5** to quinone **6** increased the antimalarial activity by more than 20-fold to an IC<sub>50</sub> of 10 μM, suggesting that the quinone functionality is essential for activity for tocopherol-related compounds. Unfortunately, following bioassays we did not have enough **4** to oxidize to the corresponding β-tocopherylquinone. This is the first report of tocopherols in red macroalgae and of antimalarial activity for tocopherols **4–6**. Furthermore, **4–6** displayed no activity in cancer and microbial assays, although **6** was not tested against human cancer cells due to insufficient material. Compounds **1** and **6** are unusual scaffolds when compared to current natural antimalarial treatments, such as the quinines and artemisinins. These meroditerpene macroalgal compounds could inspire the development of novel templates for future antimalarial drugs.

## Supplementary Material

Refer to Web version on PubMed Central for supplementary material.

## Acknowledgments

This research was supported by the U.S. National Institutes of Health's International Cooperative Biodiversity Groups program (Grant No. U01 TW007401). We thank the Government of Fiji for the permission to perform research in their territorial waters and for permission to export samples. We especially thank the Roto Tui Serua and the people of Yanuca Island for facilitating this work. We thank M. Sharma and K. Feussner for extractions; T. Davenport and S. Engel for antimicrobial assays; M.C. Sullards and D. Bostwick for mass spectroscopic analyses; L. Gelbaum for NMR assistance; A. Bommarius and T. Rogers for use of their spectropolarimeter; and I. Mamajanov, A. Engelhart, and N.V. Hud for help and use of their CD spectrophotometer.

## References and Notes

1. Kaur K, Jain M, Kaur T, Jain R. *Bioorg. Med. Chem* 2009;17:3229. [PubMed: 19299148]
2. Newman DJ, Cragg GM. *J. Nat. Prod* 2007;70:461. [PubMed: 17309302]
3. Kubanek J, Prusak AC, Snell TW, Giese RA, Hardcastle KI, Fairchild CR, Aalbersberg W, Raventos-Suarez C, Hay ME. *Org. Lett* 2005;23:5261. [PubMed: 16268553]
4. Kubanek J, Prusak AC, Snell TW, Giese RA, Fairchild CR, Aalbersberg W, Hay ME. *J. Nat. Prod* 2006;69:731. [PubMed: 16724831]
5. Lane AL, Stout EP, Lin AS, Prudhomme J, Roch KL, Fairchild CR, Franzblau SG, Hay ME, Aalbersberg W, Kubanek J. *J. Org. Chem* 2009;74:2736. [PubMed: 19271727]
6. Lin AS, Stout EP, Prudhomme J, Roch KL, Fairchild CR, Franzblau SG, Hay ME, Aalbersberg W, Kubanek J. *J. Nat. Prod* 2010;73:275. [PubMed: 20141173]
7. Lane AL, Stout EP, Hay ME, Prusak AC, Hardcastle K, Fairchild CR, Franzblau SG, Roch KL, Prudhomme J, Aalbersberg W, Kubanek J. *J. Org. Chem* 2007;72:7343. [PubMed: 17715978]
8. Ohtani I, Kusumi T, Kakisawa Y. *J. Am. Chem. Soc* 1991;113:4092.
9. Frelek J, Klimek A, Ruskowska P. *Curr. Org. Chem* 2003;7:1081.
10. Gorecki M, Jablonska E, Kruszewska A, Suszczynska A, Lipkowska ZU, Gerards M, Morzycki JW, Szczepek WJ, Frelek J. *J. Org. Chem* 2007;72:2906. [PubMed: 17375957]
11. Shin TS, Godber JS. *J. Chromatogr. A* 1994;678:49.
12. Melchert HU, Pollok D, Pabel E, Ruback K, Stan HJ. *J. Chromatogr. A* 2002;976:215. [PubMed: 12462612]
13. Reddy P, Urban S. *Phytochemistry* 2009;70:250. [PubMed: 19155027]
14. Amico V, Oriente G, Piattelli M, Ruberto G, Tringali C. *Phytochemistry* 1982;20:421.
15. Munne-Bosch S, Alegre L. *Crit. Rev. Plant Sci* 2002;21:31.
16. Niki E. *Redox Rep* 2007;12:204. [PubMed: 17925092]

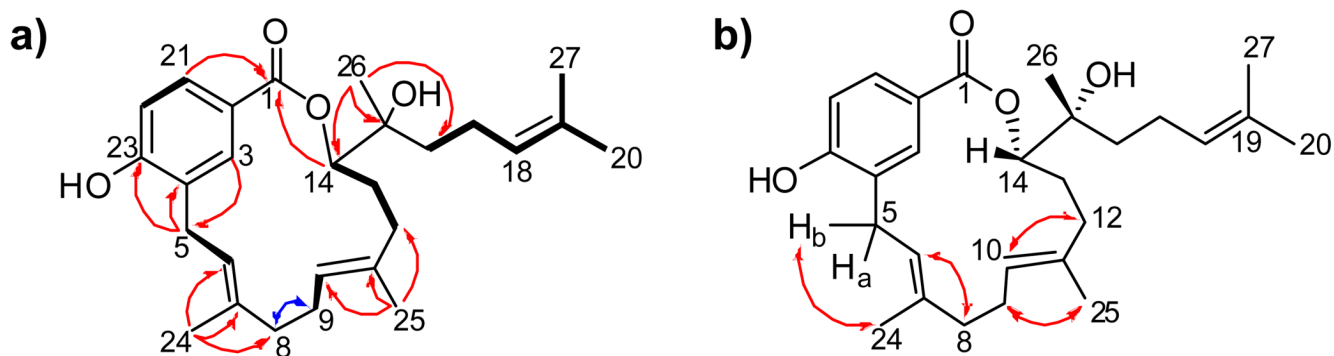


**Figure 1.** Key 2D NMR spectroscopic correlations establishing the connectivity of callophycolide A. **a)**  $^1\text{H}$ - $^1\text{H}$  COSY (bold), HMBC (red single-headed arrows), and HSQC-TOCSY (blue double-headed arrow) correlations; **b)** ROESY (red double-headed arrows) correlations establishing configurations for macrocyclic olefins in **1**.

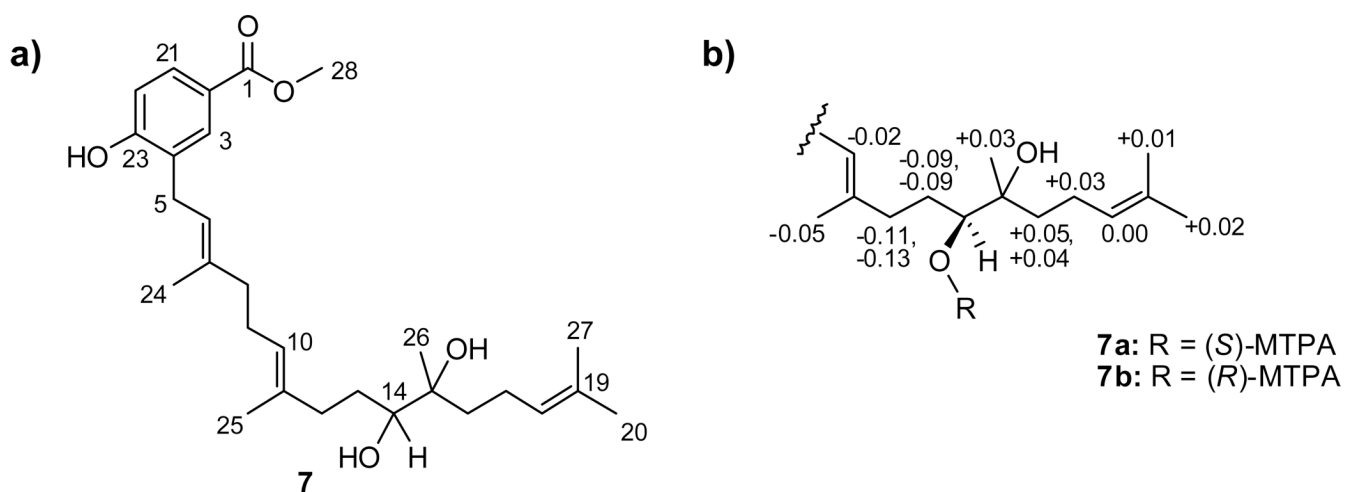


**Figure 2.** Mosher's ester analysis of callophycolide A (**1**). **a)** Methanolysis product **7**; **b)** and  $\Delta\delta_{S-R}$  values (ppm) for Mosher esters **7a** and **7b** from **7**.

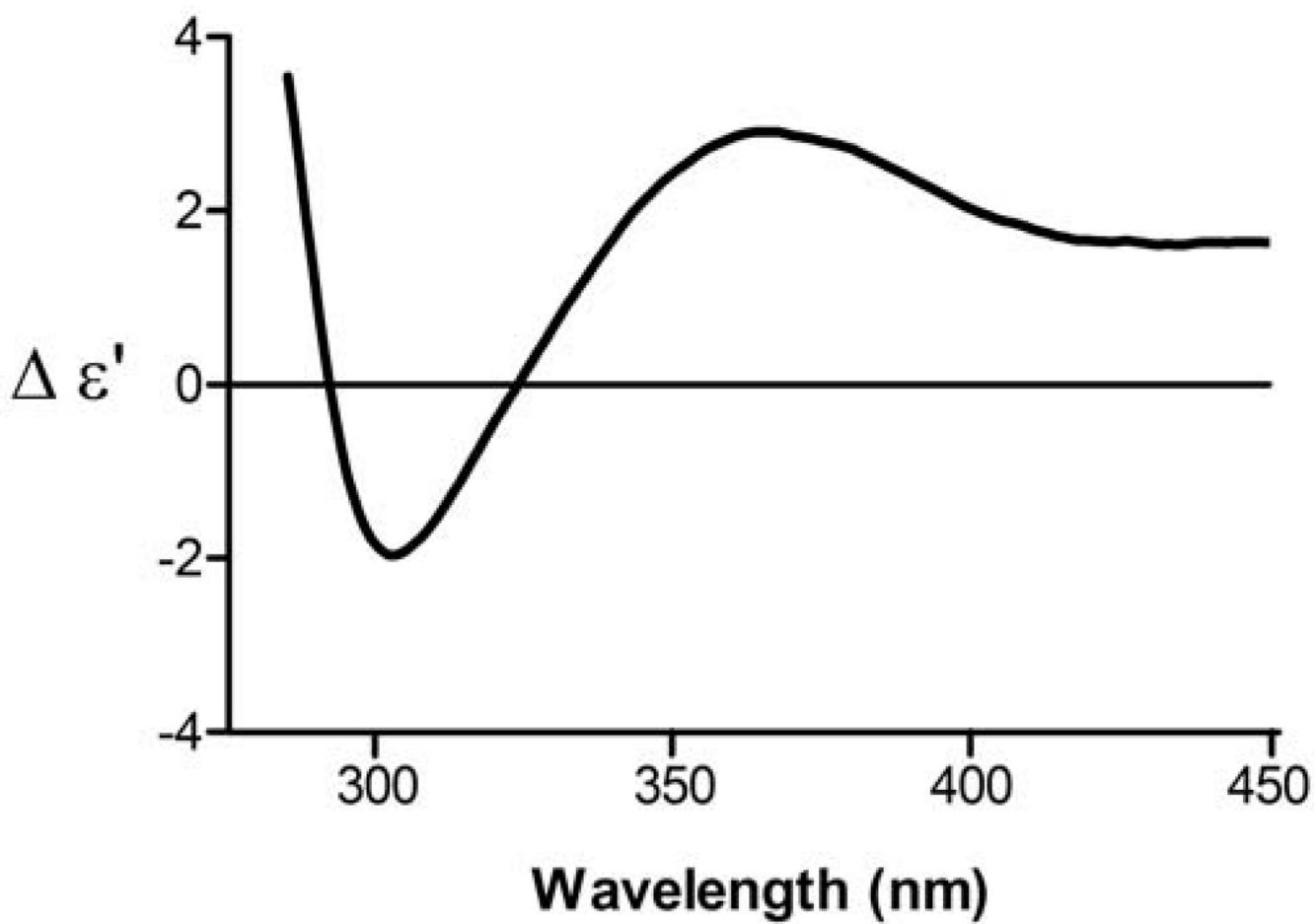


**Figure 3.** CD spectrum of the *in situ* Mo<sub>2</sub>-complex formed with methanolysis product 7.



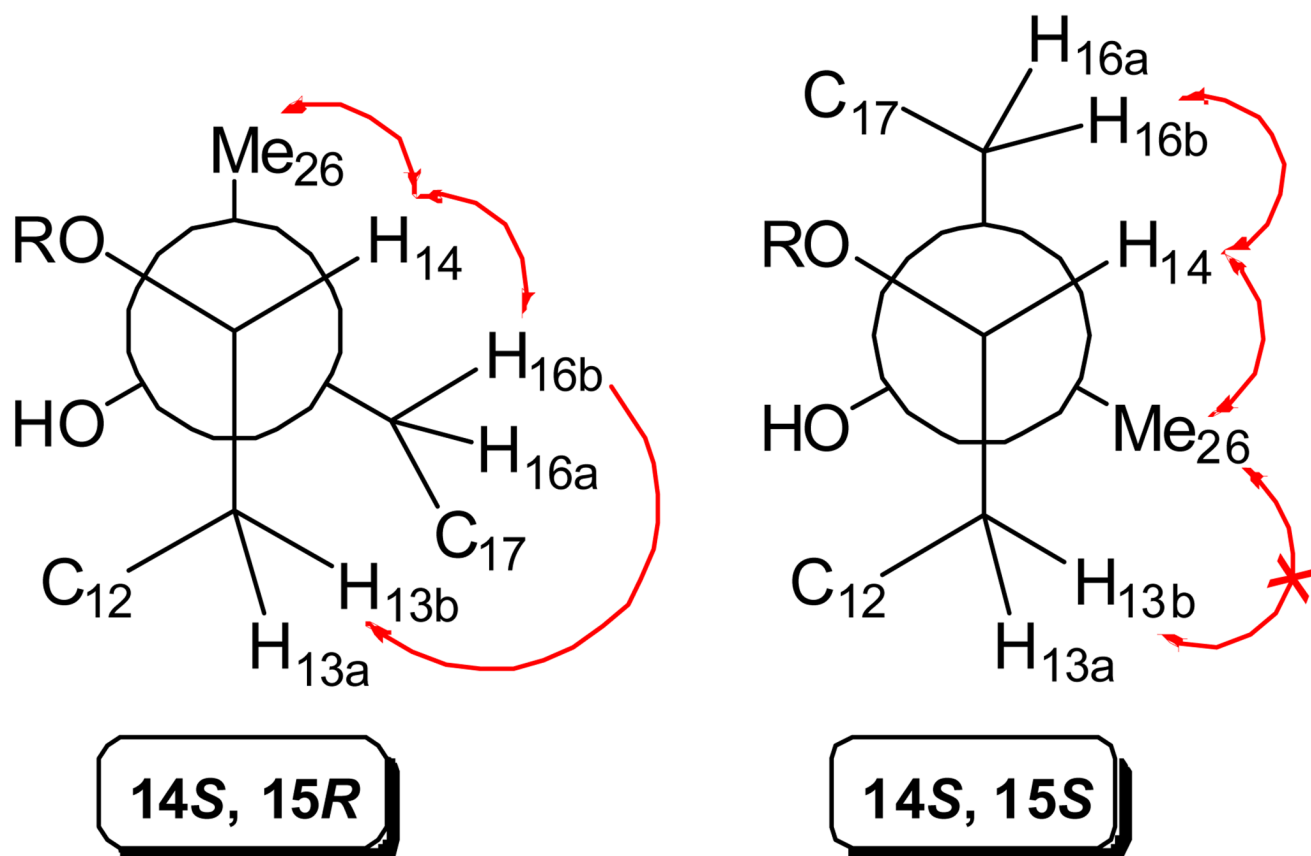


**Figure 4.** Observed NOE correlations (ROESY = double-headed arrow; 1D NOE = single-headed arrow) used to establish the relative stereochemistry at C-15 as *R* in **1**. NOEs that were not observed are indicated by an “x” through the arrow.

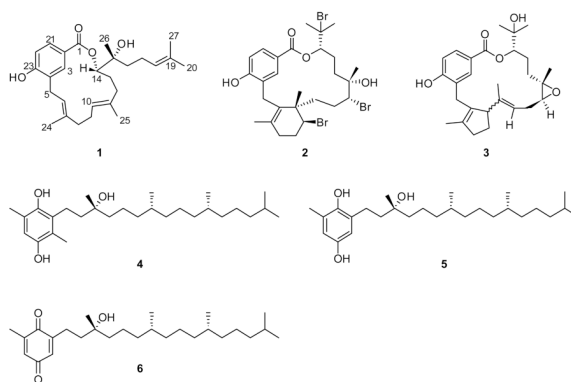


Table 1

Pharmacological activity of **1–6**. Biological activities for **2–3** were reported previously.<sup>3,5</sup>

compd.	antimalarial activity		antimicrobial MIC (μM)			
	IC <sub>50</sub> (μM)	IC <sub>50</sub> (μM) <sup>a</sup>	MRSA <sup>b</sup>	VRE <sup>c</sup>	<i>M. tuberculosis</i>	ARCA <sup>d</sup>
<b>1</b>	5.2	18	9.1	9.1	12	>250
<b>2</b>	0.7	6.7	5.9	5.9	11	49
<b>3</b>	>100	>76	NT	NT	>100	>500
<b>4</b>	190	>25	>500	>500	NT	NT
<b>5</b>	220	>25	>500	>500	>100	NT
<b>6</b>	10	NT	>500	>500	NT	>500

<sup>a</sup>Median of 12 cell lines

<sup>b</sup>Methicillin-resistant *Staphylococcus aureus*

<sup>c</sup>Vancomycin-resistant *Enterococcus faecium*

<sup>d</sup>Amphotericin B-resistant *Candida albicans*

NT indicates not tested due to insufficient material